The use of the tracker in the CMS trigger

M.A. Vos [??,??]

[a] *INFN - sezione di Pisa, Largo Pontecorvo 3, Pisa, Italy*
[b] *currently at IFIC, Apd. Correos 22085, Valencia, Spain*

Abstract

The CMS trigger stands for the daunting task of selecting rare signal processes amidst the 40 Million bunch crossings per second of the LHC. While information from the tracker is not available in the first hardware trigger level, reconstructed tracks play a crucial role in the subsequent High Level Trigger. In this contribution an overview is given of the design and performance of track reconstruction, vertexing and online selection algorithms that have been developed within the collaboration. Then, an outlook towards the even more challenging situation in the luminosity upgrade of the LHC (known as super-LHC). Two proposals to employ the tracker information in the first level selection are briefly outlined.

Key words: High Level Trigger, CMS, tracker

1. Introduction

The Large Hadron Collider at CERN is designed to explore the energy frontier. The machine is designed to deliver proton-proton collisions with an a beam energy of 14 TeV and a luminosity of $2 \times 10^{33} cm^{-2} s^{-1}$ in the initial phase, growing to the design value of $1 \times 10^{34} cm^{-2} s^{-1}$. The online selection of rare signal events among the overwhelming background production is an unprecedented challenge.

The CMS detector has a large, all-silicon tracker in a 4 Tesla solenoidal field for precise measurement of the transverse momentum of charged particles. Close to the interaction point a pixel detector consisting of three pixel barrel layers at radii of 4, 7 and 10 cm and two pixel disks in each end-cap provides precise 2-dimensional space points. The central silicon strip tracker consists of four Tracker Inner Barrel cylinders up to a radius of 55 cm, and 6 Tracker Outer Barrel cylindrical layers out to $R = 110$ cm. Hermetic coverage up to a pseudo-rapidity of 2.5 is ensured by three Tracker Inner Disks and nine Tracker End Cap disks on each side. The tracker information is complemented by an Electromagnetic and Hadronic calorimeter and an outer tracking system for muons.

The CMS trigger in figure **??** consists of two distinct levels. The first stage, known as first level trigger or L1, is entirely implemented in custom hardware. It performs a rapid (latency of the order of 3 μs) decision on the basis of information from the calorimeters and muon chambers, reducing the event rate to the level of 100 kHz. Throughout the L1 latency, the tracker information is buffered on the Front End electronics.On receipt of a L1 trigger signal the (sparsified) analog data from 60 million

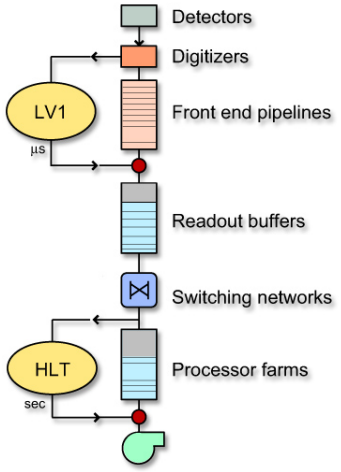

Fig. 1. Schematic representation of the CMS trigger architecture

pixels and from over eight million SST channels is shipped to the Front End Drivers and digitized.

The second trigger level, the High Level Trigger or HLT, has access to the complete event information including that from the tracker. The HLT reconstruction and selection algorithms are implemented in software and run on a large filter PC-farm. This provides a flexible environment in which the HLT can benefit from algorithms of arbitrary complexity. Importantly, there are no separate trigger levels within the HLT. Several trigger streams corresponding to different HLT objects are scheduled to run independently. To reduce the 100 kHz input rate to the 100-150 Hz of events written to persistent storage.

In this contribution, an overview is given of the role of the CMS tracker in several important algorithms of the High Level Trigger selection. In section **??** the track reconstruction algorithms developed for use in the HLT are introduced. The reconstruction and selection steps for the most important trigger objects are outlined in section **??**. In section **??** the expected trigger performance is briefly discussed. This contribution concludes with an outlook toward the luminosity upgrade of the LHC. In section **??** two proposals for including tracker information in the first level are introduced.

A very detailed description of the CMS trigger strategy and expected performance can be found in the collaboration's trigger and data acquisition Technical Design Report **?**. More recent information is found in **??**.

A lively discussion concerning the R & D for SLHC is found in the minutes of the CMS SLHC workshops **?**.

2. Online track reconstruction

In the CMS HLT environment, algorithms of arbitrary complexity can in principle be implemented. The most severe constraint is posed by the available CPU time. Two algorithms are employed to reconstruct high-quality tracks at a minimum computing load **??**.

An important speed-up is achieved by performing track reconstruction in regions-of-interest identified by previous trigger level. In this case only a sub-set of the event data is accessed. Thus, the combinatorial Kalman Filter track finder (or CKF, the default CMS offline algorithm) can be used in the later stages of the HLT. Several parameters of the algorithm are tuned for the online application. Where for offline applications an infinitesimal increase in efficiency is often preferred over a gain in execution speed, in the HLT the balance may be quite different.

The quality of regionally reconstructed tracks is quite comparable to those reconstructed offline in terms of parameter resolution and efficiency and fake rate. These tracks play a central role in the latest stage of most HLT algorithms, where ultimate precision is needed.

The degradation of the tracking and vertexing performance due to misalignment of the tracker elements has been studied in reference **?**. For the first data up to few 100 pb^{-1} of accumulated luminosity, the tracker alignment is assumed to be known with very limited precision from engineering specifications, survey results and the laser alignment system. The relatively small pixel detector is expected to be aligned with tracks to a precision of 10 μm. At this early stage the track parameter resolution is significantly degraded with respect to perfect alignment and the tracker contribution to the HLT is likely to be compromised. After a few fb^{-1} a complete track-based alignment down to

the sensor level should be available resulting in an overall alignment uncertainty of the Strip tracker of $\sim 20\mu m$. While a dedicated analysis on the impact on the trigger efficiency is still lacking, the effect is expected to be minor.

The pixel-only track reconstruction algorithms provides tracks based on a simplified track fit of all triplets of hits in the pixel detector **?** that are compatible with a minimum transverse momentum and with the beam spot. Pixel-only reconstruction is an order of magnitude faster than the offline algorithm. Global reconstruction of all tracks with transverse momentum greater than 1 GeV/c is well within the high level trigger budget [1] . Moreover, sharing of the load of the pixel-only reconstruction between several trigger streams leads to a significant gain.

The simplified pattern recognition relies on three hits out of three pixel layers, thus posing a severe requirement on the single layer efficiency. The fake rate is rather well controlled by the three-out-of-three requirement (to the level of 10%) and can be further improved by requiring compatibility with the primary vertex. The small lever arm of the three measurements leads to a much reduced track parameter resolution in the transverse plane (p_T, d_0). Finally, sufficiently accurate error estimates are achieved for pixel-only reconstruction **?**.

Pixel-only tracks - although of limited quality - are crucial to provide fast rejection of background events in the earlier stages of the HLT.

3. HLT algorithms

In this section the online reconstruction of the most important final state objects is outlined. The emphasis is on those algorithms where the tracker plays a crucial role.

Many of the trigger streams rely on the two track reconstruction algorithm outlined in the previous section. This does not imply, however, that the streams share reconstruction steps. Where trigger streams have considerable overlap (for example for the pixel-only reconstruction), the framework allows to schedule the algorithms such that the load is shared. Where overlaps are small, as is often the case for the regional reconstruction in the later stages the HLT, the streams may be scheduled independently.

In the remainder of the text selection and reconstruction steps receive names like μ L2, e/γ L2.5, etc, suggesting the existence of separate trigger levels. It should be emphasized that these are mere labels to indicate the order of execution of the different decision steps.

Unless stated otherwise, numbers for thresholds, rates, etc. are given for the initial low-luminosity phase of the experiment.

3.1. *Muon selection*

The muon L1 trigger is based on the measurement of Cathode Strip Chambers and Resistive Plate Chambers in the return yoke of the tracker solenoid.

In the first reconstruction step (labelled μ L2) of the muon trigger stream tracks are reconstructed using a Kalman filter-based algorithm on the Drift Tube muon chamber hits. Muon identification at this stage is quite efficient and pure. The momentum resolution is of the order of 10-15 % **?** for muons from W-decay, limited by multiple scattering in the iron. Thus, the main background is from *promoted* muons: real, low-momentum muons (mostly from b or c-decay) are mis-measured to have a p_T above threshold.

In the next stage (labeled as μ L3) the muon track is extrapolated into the inner tracker. A region-of-interest is defined by the extrapolated trajectory and the interaction region. Track seeds are constructed from pairs of pixel detector hits. The full track is found by a regional application of the CKF track finder. The transverse momentum resolution for muons from W-decay determined from a combined fit to the inner tracker + muon chamber hits is 1-1.5 % **?**, depending on pseudo-rapidity.

The excellent momentum resolution of the last

[1] Timing measurements are found in references **?** and **?**. Note that these only include the pure algorithmic CPU requirement. Loading and unpacking times of the detector data, cluster reconstruction and framework overhead are to be evaluated separately.

HLT stage allows to efficiently reject *promoted* low-momentum muons, thus keeping the HLT threshold (95 % efficiency is obtained for muons with a p_T over 19 GeV/c) close to that applied at L1 (14 GeV/c).

Further rejection of non-isolated muons from b- or c-decays is possible by applying an isolation criterion. Several algorithms are available, based on a reconstruction of the energy deposits in the calorimeter or of (pixel-) tracks in a cone around the muon direction.

3.2. *Electron selection*

The first level selection of high-energy electromagnetic deposits in ECAL does not distinguish between electrons and photons. The large background of photons from π^0 decay drives the L1 threshold up to 29 GeV/c.

In the first stage of the HLT (e L2) super clusters are reconstructed in ECAL, refining the energy measurement.

In the next stage (e L2.5) the super cluster is extrapolated to the pixel detector and the pixel-only track reconstruction is invoked. The matching of the reconstructed tracks with the super clusters allows to distinguish electrons and photons.

The final (e L3) selection is based on regional CKF track reconstruction of the electron track, after which requirements on the E/P (energy deposition in ECAL versus electron momentum measured in the tracker) and H/E (hadronic versus electromagnetic energy deposition) ratios and calorimeter, pixel or tracker isolation are applied **????**.

Track reconstruction yields a large number of handles to refine the online electron selection. The electron E_T thresholds in the HLT can thus be kept at the same level as the L1 threshold (29 GeV). For photons the π^0 background is much harder to reduce and the HLT threshold is driven up to 80 GeV.

3.3. *τ-jet selection*

τ-leptons decaying to muons or electrons are efficiently triggered by the above-described streams. For the majority of hadronically decaying τ-leptons (τ-jets) a dedicated trigger is available **?**.

The L1 selection requires the presence of an energetic (95 % efficient for $E_T > 86$ GeV) calorimeter cluster. A jet veto is applied: the calorimeter cluster is accepted only if the active towers are distributed in certain narrow patterns expected for the highly collimated τ-jets.

The calorimeter reconstruction of the two most energetic L1 candidates is refined in the first HLT stage (τ-jet L2). The selection of this level is based on the isolation of the collimated τ-jet, more specifically on the energy deposition in a ring around the jet core $P_{isol} = \Sigma_{\Delta R<0.4} E_T - \Sigma_{\Delta R<0.13} E_T$, where $\Delta R = \sqrt{(\Delta\phi)^2 + (\Delta\eta)^2}$.

In the L3 selection tracks are reconstructed in a region of interest. A minimum p_T is required for the highest p_T track in a narrow matching cone (the leading track). An isolation region is defined: if the number of tracks outside a narrow signal cone around the leading track, but inside a much larger isolation cone exceeds a certain number, the τ-jet candidate is rejected. For the di-τ trigger, where sufficient rejection can be obtained with relatively loose cuts, the algorithm is fed with pixel-triplet tracks. For the single τ-jet trigger the regional CKF reconstruction is used.

A tagging efficiency of 70-80 % on τ-jets from MSSM Higgs decays ($M_H = 200$ GeV $/c^2$) for a rejection factor of 10 for the main QCD background (50-170 GeV) is achieved.

3.4. *b-jet selection*

Triggering of purely hadronic final states at the LHC is an unprecedented challenge due to the overwhelming background from QCD di-jet production. The selection of fully hadronic final states can greatly benefit from the experimental sensitivity for the presence of b jets. The copious $b\bar{b}$ production at the LHC limits the rejection that can be obtained from b-tagging to roughly a factor 20 **??**.

Events that trigger the jets or the non-isolated muon or electron L1 streams are considered as b-jet candidates and are fed to the b-jet High Level Trigger.

The first HLT stage is entirely based on the

calorimeter. A set of E_T thresholds is applied that are considerably higher than the L1 requirements, but significantly lower than the thresholds of the HLT jet trigger.

In the b-jet L2.5 stage, pixel-only tracks based on hit triplets are reconstructed in regions around the two most energetic jets in the event. The track counting b-tagging algorithm is applied: if the number of tracks with a signed impact parameter significance (measured impact parameter divided by the error estimate from the track fit, signed to give positive significance to tracks with real lifetime) over a certain value in either of the jets exceeds 2 the event passes to the next level.

The final (L3) selection is based on a regional CKF track reconstruction around the jet indicated by the previous level. The much greater precision of these tracks allows the application of a much stricter b-tagging selection.

The addition of the b-jet trigger to the CMS trigger table has resulted in a significant increase in the trigger performance for fully hadronic states containing one or more energetic b-jets, like fully hadronic decay of $t\bar{t}$ events **??**.

4. High Level Trigger performance

The performance of the CMS online selection in terms of background rate and efficiency for certain benchmark processes has been reported in great detail in references **?** and **?**. A more recent study can be found in **?**, especially in appendix E of volume II of the latter.

As an exercise to demonstrate the selection performance for the most important physics channel, a CMS *trigger table* is defined. Table **??** below presents an extract of the table for the initial low-luminosity ($L = 2 \times 10^{33}$) phase of the experiment in **?**. The entry for the b-jet trigger is from **??**. Where comparison is possible, more recent results published after the workshop in **?** generally agree very well.

A large number of triggers have not been listed in table **??**. For each of the objects (except for the jet triggers), the trigger table contains a di-object trigger with much reduced thresholds and

Table 1
Extract of the CMS trigger table as defined for the initial low-luminosity ($L = 2 \times 10^{33}$) phase of the experiment. Thresholds are given as 95 % efficiency points (90 % for muons). L1 rates contain a safety factor of 3, to take into account systematic uncertainties.

	L1		HLT	
	threshold (GeV)	bkg. rate (kHz)	threshold (GeV)	bkg. rate (Hz)
μ	14	2.7	19	25
$e^{\pm}$	29	3.3	29	33
γ	29	3.3	80	4
τ-jet	86	2.2	86	3
1,3,4-jet	177, 86, 70	3.0	657,247,113	9
b-jet	177, 86, 70	3.0	350,150,55	17

allocated rate. The HLT di-muon threshold is 7 GeV/c, the di-electron threshold is 17 GeV, the di-photon thresholds are 40 and 25 GeV and the di-τ-jet threshold is 59 GeV. The trigger table is further extended with cross-triggers combining different objects. Finally, algorithms have been developed for several types of calibration triggers, for B-physics triggers, etc.

For LHC data taking at the design luminosity of $1 \times 10^{34} cm^{-2} s^{-1}$ the trigger table is modified to cope with the higher background rates. While more sophisticated algorithms may help to improve the HLT performance, it is inevitable that the first level trigger thresholds for single objects are raised: in reference **?** for e/γ, μ and τ triggers the p_T increase from 29 GeV to 34 GeV, from 14 to 19 GeV and from 86 to 101 GeV, respectively.

5. Outlook toward the luminosity upgrade (SLHC)

While online selection in the LHC at design luminosity is definitely challenging, a redesign of the trigger strategy may be required for the envisaged luminosity upgrade of the accelerator (SLHC). One example is often brought up: due the limited momentum resolution of the CMS L1 muon chambers for high p_T muons, raising the L1 threshold over 20 GeV leads to very small reduction of the back-

ground rate. It seems clear that the CMS L1 needs greater momentum resolution in the range 20-50 GeV to cope with the SLHC rate and keep the thresholds at an acceptable level.

Within the CMS collaboration, several proposals to incorporate the tracker in the L1 trigger decision have been put forward in recent years **????**. Combination of the muon trigger chambers with a few precision measurements in the tracker is expected to drastically reduce the background rate. Two proposals are briefly outlined here.

Stacked pixel layers **?** consist of two fine granularity pixel detectors ($R\phi$ dimension of the pixels is of the order of 20 μm), stacked with a spacing of the order of a few mm. With an assumption on the origin of the track (beam constraint) hits from the two stacked layers can be paired unambiguously: track stubs (hit pairs) can thus be formed while avoiding large pairing combinatorics in the dense tracking environment.

Depending on the inner radius of the stack, the stack spacing and the granularity, hit pairs in the closely stacked layers have a certain sensitivity to the track p_T. Performing a nearest neighbor search in the inner sensor seeded by the hit in the outermost sensor of the stack, turn-on curves as in figure **??** may be obtained. Thus, hit pairs corresponding to high p_T tracks can effectively be selected, allowing a large reduction of the data volume to be shipped off-detector.

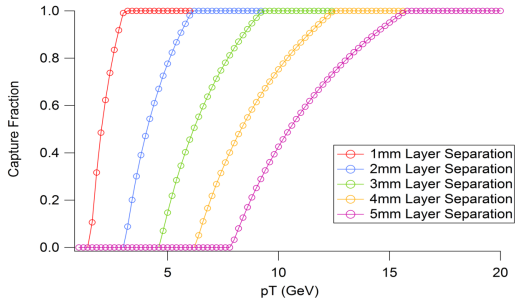

Fig. 2. Turn-on curves for two stacked pixel layers with an $R\phi$ pixel size of 20μm at a radius of 10 cm from the interaction point. The leftmost curve corresponds to a stack spacing of 1 mm, the rightmost curve to 5 mm.

The stacked layer approach thus alleviates two of the outstanding problems for incorporating tracker information in the L1 decision, both the track candidate combinatorics and the data rate are reduced to a manageable level. On the other hand, the approach implies a challenge in a number of areas: the sensor technology, implementation of the correlation logic and the mechanical constraints are currently being studied.

A second proposal **?** aims to implement part of the current HLT selection based on high-quality tracks - with a p_T resolution well below 10 % for track p_T in the 20-30 GeV range - into the first level trigger. To unambiguously reconstruct tracks with the required precision, a relatively large (4-6) number of low-occupancy points is needed with a large lever arm.

It is therefore proposed to bring out the zero-suppressed data of the layers at intermediate radii (20 - 50 cm) for off-detector processing in a highly parallel hardware architecture. This proposal builds on the evolution of *proven* technology. The current hybrid pixel technology with large cell sizes yields sufficient space point resolution. Simulation of the occupancy and data volume **?** show that data transmission may well be manageable using the digital opto-links currently in use in the ATLAS SCT. For off-detector processing a highly parallel architecture is envisaged, consisting of an FPGA switch distributing the information of each trigger tower (ϕ-slice) to a large number of Associative Memories (a la SVX in CDF **?**). Thus, efficient reconstruction of tracks above a large p_T threshold ($5 - 15$ GeV) can be achieved in the limited time available.

While this second proposal is quite conservative as far as the requirements on the sensor are concerned, the development of on-detector electronics, data links and the off-detector processing that can cope with the data rate and the latency pose a serious challenge. Detailed feasibility studies are currently being performed.

Figure **??** shows how the availability of a precise momentum measurement leads to a very significant reduction of the SLHC L1 rate for single muons.

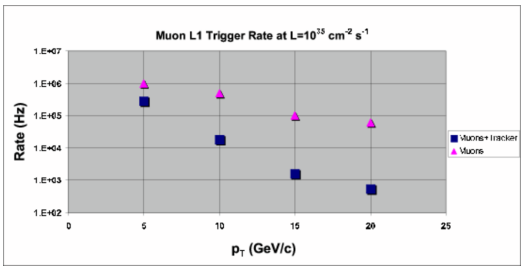

Fig. 3. Single muon L1 trigger rate at the SLHC. Triangles: muon system stand-alone. Squares: combined measurement of the muon system + L1 tracker trigger as outlined in the text.

6. Summary

Two main strategies are followed to bring track reconstruction CPU requirements within the scope of the HLT: for fast rejection of background events in the earliest stage of the trigger triplets of pixel detector hits are reconstructed. At a later stage tracks with close to offline quality are available thanks to a regional application of the Combinatorial Kalman Filter algorithm.

The tracker plays a crucial role in many of the selection algorithms developed for the CMS High Level Trigger. The single-lepton p_T thresholds remain close to those applied at the first level. Online tagging of b- and τ-jets leads to a significantly improved trigger efficiency for hadronic final states containing b- or τ-jets.

Several proposals exist to incorporate the tracker information into the L1 decision for the luminosity upgrade of the LHC (super LHC). In this contribution two proposals have been discussed with very complementary requirements for the detector R & D: while the stacked pixel layers rely on the development of novel, highly granular pixel sensors and detector combination logic, for the second the main challenge is in the development of sufficiently fast on-detector and off-detector electronics and data links.

References

The CMS collaboration., CERN/LHCC 2002-26
W. Adam et al., Eur.Phys.J.C46:605-667,2006.
The CMS collaboration. CMS physics Technical Design Report, volume I (CERN-LHCC-2006-001) and II (submitted August 2006).
The 4th CMS workshop on Detectors and Electronics for the SLHC, Perugia, Italy, April 2006
M. Vos for the CMS collaboration, CMS-CR-2006-004, Nucl.Instrum.Meth.A566 (2006) 174-177.
T. Boccali for the CMS collaboration, Nucl.Instrum.Meth.A511 (2003) 150-152.
P. van Laer et al., Impact of CMS Silicon Tracker Misalignment on Track and Vertex Reconstruction, CMS-NOTE-2006-029
S. Cucciarelli, M. Konecki, D. Kotliński, T. Todorov, CMS Note 2003/026
S. Baffioni et al., CMS-NOTE-2006-040.
P. Govoni for the CMS collaboration, Nucl.Phys.Proc.Suppl.150 (2006) 295-298.
G. Bagliesi et al., CMS-NOTE-2006-028.
M. Vos, F. Palla, CMS-NOTE-2006-030.
D. Benedetti, L. Fano, M. Biasini, Nucl.Phys.Proc.Suppl.142 (2005) 426-429.
M. Davids et al., CMS NOTE 2006/077
C. Foudas, A. Rose, J. Jones, G. Hall, LECC 2005, physics/0510227
J. Jones, G. Hall, C. Foudas, A. Rose, physics/0510228
F. Palla, LECC 2006, CMS CR-2006/087, submitted for publication.
M. DellOrso and L. Ristori, Nucl. Intsr. Meth., vol. A278, no. 2, pp. 436-440, Jun. 1989.